Video Article

Photothrombosis-induced Focal Ischemia as a Model of Spinal Cord Injury in Mice

Hailong Li*[1], Gourav Roy Choudhury*[1], Nannan Zhang[1], Shinghua Ding[1]

[1]Department of Bioengineering, Dalton Cardiovascular Research Center, University of Missouri

*These authors contributed equally

Correspondence to: Shinghua Ding at dings@missouri.edu

URL: https://www.jove.com/video/53161
DOI: doi:10.3791/53161

Keywords: Medicine, Issue 101, Spinal cord injury, photothrombosis, Rose Bengal, ischemia, epi-fluorescent microscopy, reactive gliosis, infarct, paraplegia

Date Published: 7/16/2015

Citation: Li, H., Roy Choudhury, G., Zhang, N., Ding, S. Photothrombosis-induced Focal Ischemia as a Model of Spinal Cord Injury in Mice. *J. Vis. Exp.* (101), e53161, doi:10.3791/53161 (2015).

Abstract

Spinal cord injury (SCI) is a devastating clinical condition causing permanent changes in sensorimotor and autonomic functions of the spinal cord (SC) below the site of injury. The secondary ischemia that develops following the initial mechanical insult is a serious complication of the SCI and severely impairs the function and viability of surviving neuronal and non-neuronal cells in the SC. In addition, ischemia is also responsible for the growth of lesion during chronic phase of injury and interferes with the cellular repair and healing processes. Thus there is a need to develop a spinal cord ischemia model for studying the mechanisms of ischemia-induced pathology. Focal ischemia induced by photothrombosis (PT) is a minimally invasive and very well established procedure used to investigate the pathology of ischemia-induced cell death in the brain. Here, we describe the use of PT to induce an ischemic lesion in the spinal cord of mice. Following retro-orbital sinus injection of Rose Bengal, the posterior spinal vein and other capillaries on the dorsal surface of SC were irradiated with a green light resulting in the formation of a thrombus and thus ischemia in the affected region. Results from histology and immunochemistry studies show that PT-induced ischemia caused spinal cord infarction, loss of neurons and reactive gliosis. Using this technique a highly reproducible and relatively easy model of SCI in mice can be achieved that would serve the purpose of scientific investigations into the mechanisms of ischemia induced cell death as well as the efficacy of neuroprotective drugs. This model will also allow exploration of the pathological changes that occur following SCI in live mice like axonal degeneration and regeneration, neuronal and astrocytic Ca^{2+} signaling using two-photon microscopy.

Video Link

The video component of this article can be found at https://www.jove.com/video/53161/

Introduction

Traumatic spinal cord injury (SCI) is a devastating clinical condition affecting the sensorimotor and autonomic functions of the SC. Patients surviving SCI are often left with debilitating paraplegia that significantly affects their daily activities and quality of life[1]. Experimental SCI models have been an indispensable tool in the scientific investigation to understand the pathophysiology of SCI and associated neural repair processes. These models have also been used to test the preclinical efficacy of various experimental neuroprotective interventions that are aimed at functional recovery. Currently, majority of the SCI models in practice employ the use of physical blunt force to mechanically disrupt and injure the SC. These methods include contusion, compression, dislocation and transection of the SC[2]. It has been suggested that after the primary mechanical insult a secondary injury in the form of ischemia sets in in the injured SC[3,4]. The etiology of secondary ischemia includes extensive tissue degeneration, parenchymal hemorrhage and sometimes by obstruction of blood vessels by tissue edema[5-7]. As a result of the secondary injury the integrity of SC is further affected, neurons and glial cells are severely impaired in function and viability and undergo apoptosis which leads to infarct growth during the chronic stage of injury, analogous to the growth of ischemic penumbra following stroke[8,9]. Several mechanisms like excitotoxicity, free radical production, and inflammation have been reported to be responsible for the ischemic cell death following SCI[10,11]. In addition, SC ischemia is a serious complication of thoraco-abdominal aortic aneurysm repair surgeries which often lead to paraplegia in the patients[12,13]. In spite of such high clinical impact very few models of spinal cord ischemia with high reproducibility are currently available.

Photothrombosis (PT) is a commonly used method for the induction of focal ischemia in the brain[14-20]. The technique is fairly non-invasive, highly reproducible and produces a precise focal ischemic lesion in the exposed area of the brain[17-21]. This is achieved by systemic administration of photoactive dyes like Rose Bengal (RB)[16-20,22] or erythrosine B[23] followed by localized irradiation of blood vessels with proper light source. Photoactivation of the dye causes the generation of free radicals which disrupt the integrity of the smooth vascular endothelium, and cause the platelets to accumulate, which subsequently forms a thrombus. The obstruction of blood flow by the thrombus results in an infarct in the region supplied by the vessel[24]. Due to ease of control on the intensity and duration of irradiation this procedure yields a highly uniform and reproducible infarct. Furthermore, this method can be employed to induce an infarct at various anatomical locations enabling spatial (*e.g.*, grey matter vs. white matter) understanding of the effect of ischemia.

The aim of the current study is to develop an easy and highly reproducible model of SC ischemia in mice. We described the procedure of a PT model of SC ischemia in mice. Results from histology and immunostaining demonstrated that PT can effectively induce SC infarction, neuronal loss and reactive gliosis.

Protocol

Note: Mice (C57BL/6J, male) aged 10 – 12 weeks were used in this study. All the procedures were performed in accordance with the NIH Guide for the Care and Use of Laboratory Animals and were approved by the University of Missouri Institutional Animal Care and Use Committee (IACUC).

1. Pre-Surgery

1. The day before surgery autoclave and sterilize all the surgical instruments. Wrap the instruments and autoclave at 121 ^{o}C at 15 psi for 30 min followed by 30 min of drying (121 ^{o}C, 15 psi, 30/30 cycle). Place the instruments in a clean and sterile environment until further use.
2. Prepare fresh Rose Bengal (RB) solution (20 mg/ml in sterile saline) every time before the surgery. To completely dissolve RB, vortex the tube then followed by sonication for 5 min at 50/60 Hz with output power of 19 W. Wrap the tube in aluminum foil and protect it from light until further used during surgery.
3. Prepare a mixture of ketamine/xylazine in sterile saline. Add 125 µl of xylazine (stock concentration: 20 mg/ml) and 325 µl of ketmaine (stock concentration: 100 mg/ml) and 550 µl of sterile saline to make a final volume of 1 ml of anesthetic mixture.
4. Pre-warm the homeothermic heating pad.
5. Pre-warm the metal halide lamp (light source for FN1 epi-fluorescence microscope) for 30 min to stabilize the lamp power.
6. Adjust the size of the illuminated region to a diameter of 1 mm using 10X objective and a reticle by adjusting the field diaphragm in the upright FN1 epi-fluorescence microscope.

2. Surgical Procedure

1. Anesthetize the mouse with a dose of ketamine (130 mg/kg B. wt.) and xylazine (10 mg/kg B. wt.). Based on the cocktail in 1.3, 4 µl per g of mouse B. wt. are needed. Sterilize the site of injection with an alcohol swab and administer the anesthetics through the intra-peritoneal (IP) route. Take care not to inject the anesthetics into the blood vessels or muscle as this would delay the induction and recovery of the animal.
2. Apply artificial tear ointment to both eyes of the mouse to prevent drying and place the animal on the heating pad to prevent hypothermia.
3. Preparation of animal
    1. Check the animal for proper surgical level anesthesia by using the toe pinch response.
    2. Once the animal has reached surgical level of anesthesia, clip the hair on the dorsal surface around midline of the animal using an electric hair trimmer. Scrub the surgical site with 70% ethanol followed by betadine solution three times. Cover the site with a sterile surgical drape until next step.

4. Surgical procedure to thin the bone to expose the spinal cord
    1. Place the mouse in a prone position over the homeothermic heating pad on the surgical platform (**Figure 1A**). Properly secure the mouse posture using a snout clamp to maintain an elongated neck region (**Figure 1A, B**).
    2. Make an incision (approximately 1 cm long) using surgical scissors along the dorsal mid line extending from the thoracic vertebrae T9 to T12. Move aside the skin to expose surgical area.
    3. Using a scalpel, carefully clear the muscle to expose the dorsal spines at T9 - T12 vertebrae. Stop bleeding in each step by applying gentle pressure with sterile cotton swab. Separate T10 - T12 vertebrae from the surrounding muscle and secure them using a vertebral clamp to stabilize and prevent any movement (**Figure 1A, B**).
    4. Using a high speed drill with bone polishing drill bit, carefully and gently thin the dorsal surface of T10 or T11 vertebra to visualize the posterior spinal vein and other small vessels on the dorsal surface of the SC (**Figure 1C**).
    5. To prevent thermal damage due to heat generated during the thinning procedure, apply a gentle and constant stream of normal saline along with constant suction to remove the debris.
    6. Using a scalpel carefully smooth the bone surface until the main vessel is clearly visible. Take care not to damage the spinal cord during this process.
    7. Once the blood vessel is visualized, administer RB at a dose of 30 mg/kg (body weight) through retro-orbital sinus route using an insulin syringe.
    8. Measure blood flow using a Laser Doppler flowmeter after 3 min following RB injection if necessary (**Figure 2A, B**). Maintain asepsis during entire procedure.

3. Induction of PT

1. Place the animal on an X-Y position adjustable stage over a Lab-Jack which can adjust the height. Adjust the position of the mouse so the exposed region of T11 spinal cord is directly under the 10x objective of the FN1 epi-fluorescence microscope (**Figure 3A**).
2. Set the power of the light source at 12% and irradiate the T11 region with a diameter of 0.75 mm in the middle of thinned spinal cord (Note: this region includes the posterior spinal vein and other capillaries) with a green light (wavelength 540 - 580 nm, which is achieved by the filter cube in the microscope) through the 10X objective for 2 min. Take images at the beginning and end of irradiation (**Figure 3B, C**) and record the time of the experiment at this point.
3. Measure blood flow again for 10 min if necessary by placing the laser Doppler probe to the same position above the spinal cord as in 2.4.8 (**Figure 2A, B**).

4. After irradiation check for any hemorrhage and if none found proceed to suturing the animal. Suture the superficial fascia along with the muscles on the either side of spinal cord using an absorbable suture or 4-0 size silk suture. Take care not to damage the exposed SC. Suture the skin with 4-0 silk suture. Apply Betadine or iodine to the edges of the skin after suturing.

4. Post-surgery Care

1. After suturing, place the animal on the heating pad for recovery. After recovery check the animals for signs of neurological deficits by observing the movement of both hind-limbs. Do not leave the animal unattended until it has regained sufficient consciousness to maintain sternal recumbency.
2. Transfer the animals to the home cage. Do not return the animal that has undergone surgery to the company of other animals until fully recovered.
3. Check the animals at regular intervals. In case of severe neurological deficits, provide proper care like evacuation of bladder, administration of analgesics (buprenorphine, 0.05 - 0.1 mg/kg). Check for dehydration and administer normal saline subcutaneously in severe case. Usually, buprenorphine (0.1 mg/kg) will be administered after suturing to relieve pain in the surgical site.
4. If animals are not immediately euthanized after surgery, we will put high water content diet on the cage floor, so the animals can reach the food easily.

5. Transcardial Perfusion, Nissl staining and Immunostaining

1. Transcardially perfuse the animal as described previously[17-20].
    1. Anesthetize the animal as described earlier in the protocol and transcardially perfuse with phosphate buffer saline (PBS, pH 7.4), followed by ice-cold 4% paraformaldehyde (PFA) in PBS.
    2. After perfusion, remove the spinal cord (SC) and post-fix it in 4% PFA in PBS at 4 °C O/N. Transfer the fixed SC into PBS with 30% sucrose and keep it for 2 - 3 days until it sinks to the bottom of the tube.
    3. Using a cryostat cut the spinal cord into 30 µm thick sections and place them serially on a gelatin-coated glass slides or in a 48-well plate with 0.01 M PBS.

2. Nissl staining: To inspect the injury caused by PT perform a Nissl staining on spinal cord sections as previously described[17-20].
    1. Briefly, collect every fifth spinal cord slice on the glass slides and stain with 0.25% cresyl violet. Take images of the stained sections (**Figure 4**).

3. Immunostaining: As described previously using a floating section method[17,18,20].
    1. Briefly, stain the spinal cord sections by incubating O/N at 4 °C with rabbit anti-glia fibrillary acidic protein (GFAP) polyclonal antibody (1:300), rabbit anti-NeuN antibody (1:300), and rabbit anti-Iba1 antibody (1:500) followed by donkey anti rabbit Alexa 568-conjugated IgG (1:400) secondary antibodies for 4 h at RT. Take images with a fluorescent microscope (**Figure 5)**.

Representative Results

The aim of this study was to produce spinal cord ischemia in mice using a PT model. After the desired region of bone above the spinal cord (T10 - T12) was thinned, Rose Bengal was injected through retro-orbital sinus route, and ischemia was induced by PT. **Figure 1A, B** show the mouse positioned in a custom-made surgical platform during surgery. The mouse was held in place by a snout clamp and two adjustable vertebrate clamps to stabilize the spinal cord. **Figure 1C** show a thinned window above the spinal cord of T10 - T12. The main blood vessel and its branches can be clearly visualized. To confirm the induction of ischemia, changes in blood flow was measured using a laser Doppler flowmeter before and after PT (**Figure 2A, B**). For analysis, the decrease in % of blood flow was calculated using the baseline blood flow before photothrombosis. Blood flow dropped to ~20% immediately after light illumination as compared with the basal level prior to illumination. **Figure 3B, C** shows fluorescent images of spinal cord blood vessels at the beginning and the end of PT. Illumination for 2 min induced blood clot in the blood vessels (**Figure 3C**), suggesting the induction of ischemia, consistent with the measurements of the laser Doppler flowmeter. To inspect the injury caused by PT, mice were sacrificed 3 days after PT and Nissl staining was performed. Images taken following Nissl staining showed the infarct region that can be clearly demarcated from the surrounding region, indicating spinal cord tissue damage and cell death after PT (**Figure 4**). Immunostaining was performed for NeuN, GFAP and Iba1. NeuN+ neurons were lost in the grey matter in the ischemic core (**Figure 5A**), while GFAP expression was increased in the border of ischemic core (**Figure 5B**, also see the boxed region). The Iba1+ microglia exhibited a globoid morphology (*i.e.*, an enlarged cell body with shorter and fewer processes, see the boxed region) along with increased Iba1 expression (**Figure 5C**). Although there was a tissue loss in the ischemic core region due to floating section staining, an increase in GFAP and Iba1 expression in the entire peri-infarct region can be clearly observed. These results indicate neuronal death and reactive gliosis in the penumbra after SC ischemia. On the other hand, substantial functional deficits were observed in the injured mice, *i.e.*, disabled hind-limb movement one day after PT, indicating paralysis of hind-limbs (see the **Movie**).

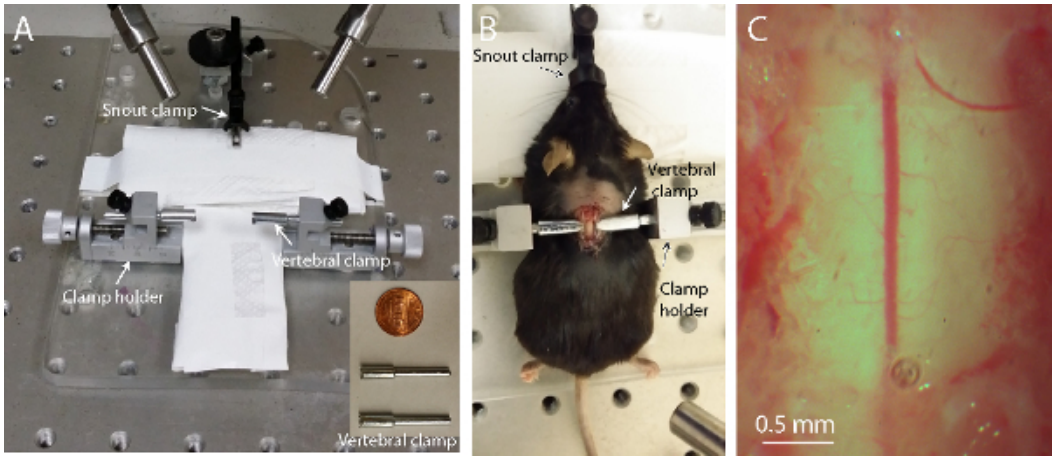

Figure 1. PT-induced ischemia model in spinal cord. (A) Photographs of the surgery platform for the spinal cord PT. Inset: enlarged vertebral clamps. **(B)** The mouse was held by a snout clamp and by two custom-made vertebral clamps on the stage. Notice that the bone was thinned at T10 - T12 region and two metal vertebral clamps were used to stabilize the spinal cord. **(C)** A zoom-in image showing the region with the thinned-bone above the spinal cord at T10-11 for the induction of PT. Notice the main blood vessels and its branches. Please click here to view a larger version of this figure.

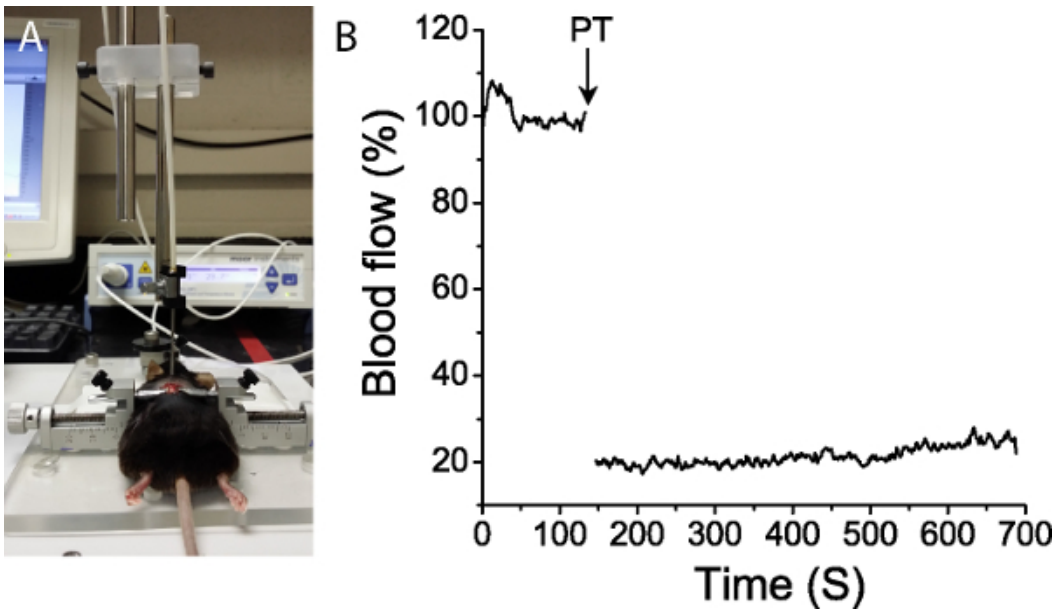

Figure 2. Spinal cord blood flow measurement. (A) The setup of the spinal cord surface blood flow measurement using a laser Doppler flowmeter and stereotaxic device to position the probe. **(B)** Spinal cord blood flow before and after PT was measured. In this experiment, PT was induced by illuminating with a light source for 2 min with a 12% power output. The diameter of the irradiated surface was 0.75 mm and was in the middle of spinal cord. Blood flow was recorded for up to 5 min to obtain stabilized signal before PT and up to 10 min following PT. Data from each mouse was normalized to the value prior to light illumination. The graph shows the averaged value of data from 3 mice. The arrow indicates the start of PT. Please click here to view a larger version of this figure.

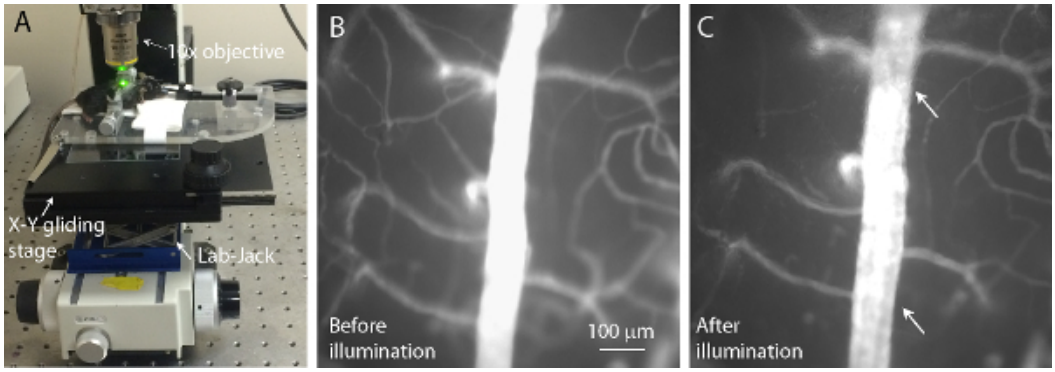

Figure 3. PT-induced spinal cord ischemia. (A) Photograph of a mouse placed on the microscope for induction PT in spinal cord. The position of the mouse can be adjusted in three dimensionally using the X-Y gliding stage and a Lab-Jack. Light from the 10X objective was focused on the surface of spinal cord. **(B-C)** Fluorescent images of the blood vessels in the spinal cord before **(B)** and after **(C)** illumination following the injection of rose Bengal. Notice the blood clot after 2 min of irradiation **(C)** (see arrows). Please click here to view a larger version of this figure.

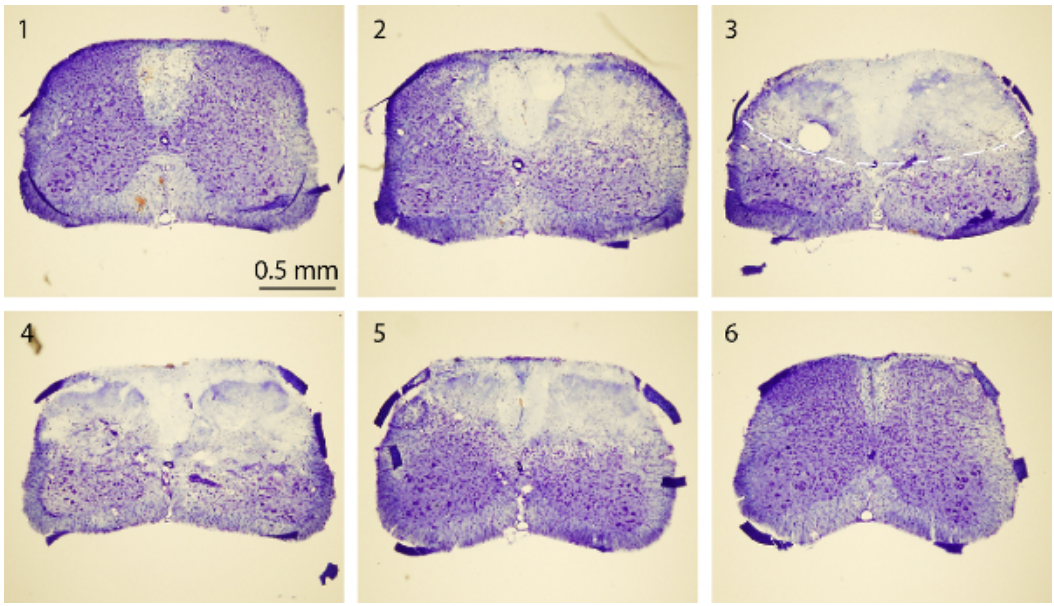

Figure 4. Nissl staining of spinal cord. Nissl staining images of a series of rostral-to-caudal spinal cord transverse sections that include normal (sections 1 and 6) and PT-induced epicenter (sections 2 - 5). The mice were sacrificed 3 days after PT. Each spinal cord section is 30 µm thick. The interval between two sections is 750 µm. The dashed line in 3rd image outlines the infarct region. Please click here to view a larger version of this figure.

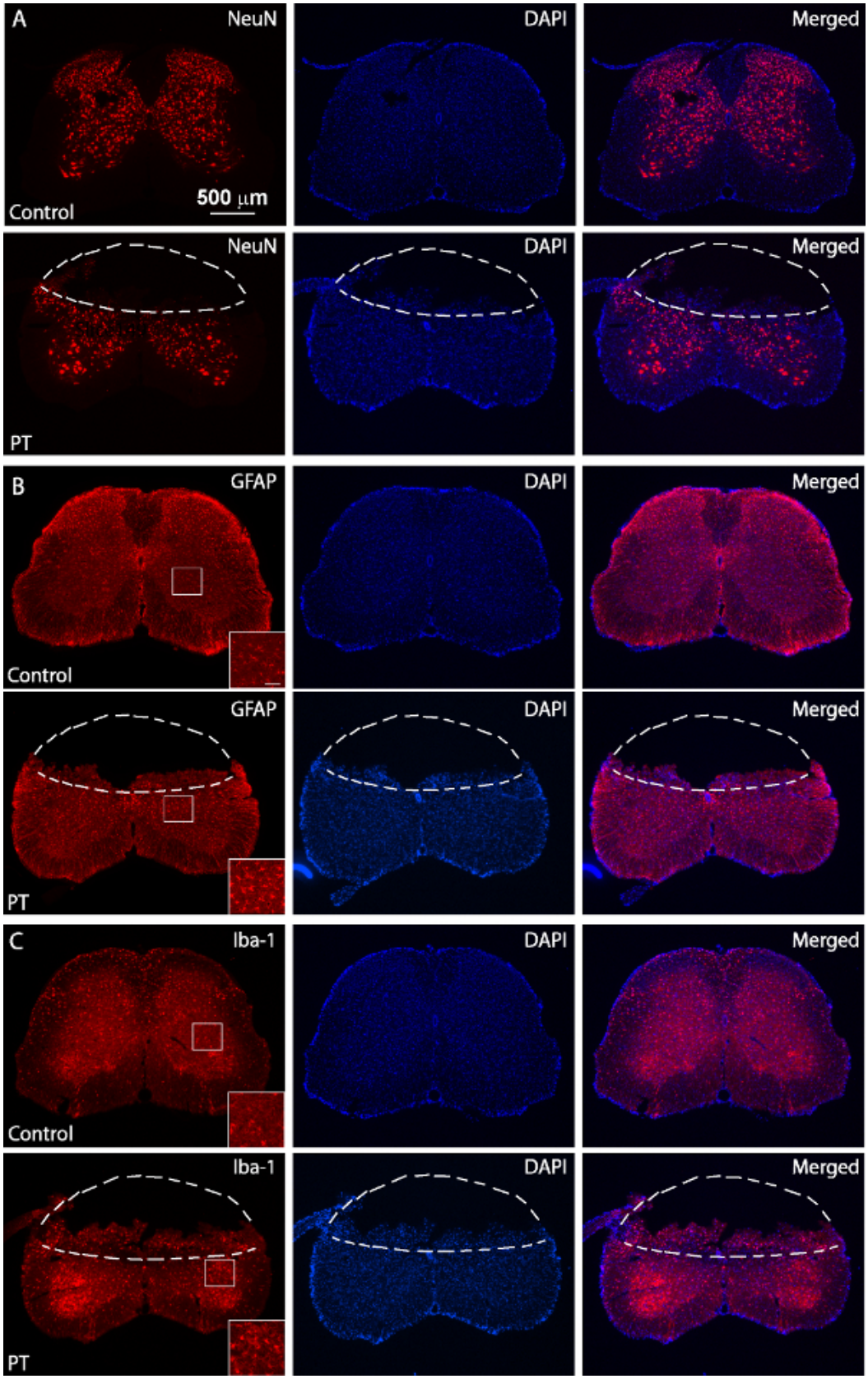

Figure 5. Immunostaining of NeuN, GFAP and Iba1. Fluorescent images of NeuN (A), GFAP (B) and Iba1(C) staining from normal (upper panels) and PT-injured (lower panels) spinal cord sections. The injured mouse was sacrificed 3 days after PT. The dashed lines separate the

infarction regions from normal tissues. The boxed regions show high resolution images of GFAP and Iba1 expression with a scale bar of 50 µm.
Please click here to view a larger version of this figure.

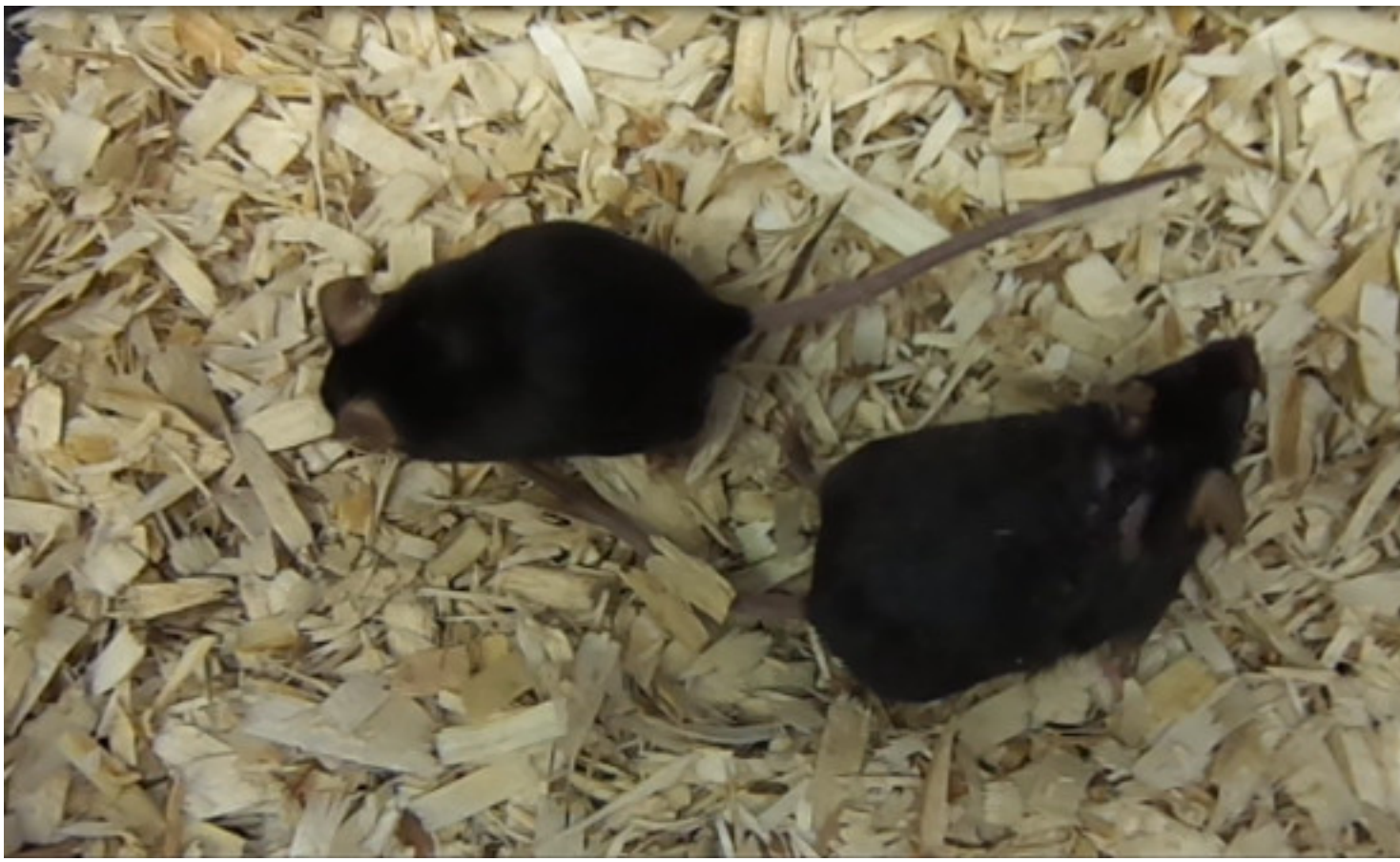

Movie. PT in spinal cord induced behavioral deficits. The movie shows the movement of a normal and a PT-injured mouse in a cage. Notice the dragging of both hind-limbs of the mouse with inured spinal cord, indicating paralysis of hind-limbs (paraplegia). The movie was taken 24 h after PT in the injured mouse.

Discussion

In this study, we described a photothrombotic model of SC ischemia. Due to advances in genetic engineering there has been a surge in commercially available transgenic mice which has made it possible to study the impact of specific genes involved in the ischemic pathophysiology in the SC. The aim of the study was to develop a reproducible mouse model of spinal cord ischemia. Here we adapted a cortical PT model to induce SCI in mice. Following surgery the posterior spinal vein and capillaries on the dorsal aspect of mice at the level of T11 thoracic vertebra were exposed. Then RB, a commercially available photoactive dye, was injected through retro-orbital sinus route to attain desired vascular distribution. The exposed blood vessel was then irradiated by a green light to induce the formation of thrombus and later on an infarct. Our results from histological and immunostaining methods showed that PT induced an infarct in the spinal cord and reactive gliosis in the peri-infarct region. Neurological deficits like hind limb paralysis were also observed. These data suggest that PT is a suitable model for studying pathophysiology and mechanisms of cell death after SCI. The critical step in the protocol is the use of a high speed drill to thin the surface of vertebra for visualization of the blood vessel on the dorsal surface of the SC. This step should be carefully performed as application of excess pressure might cause the drill to enter spinal cavity and damage the SC. On the other hand, uneven thinning might result in improper illumination and may produce irregular infarcts. To address this issue, frequent inspection of the surface of the bone under microscope after each short step of drilling is recommended to evaluate the thickness of the bone and to further assess the use of the drill. The use of sterile saline is recommended to washout the debris as well as for the better visualization of the exposed surface. Maintaining constant asepsis during entire surgical procedure, proper post-surgical care of the animal can improve animal survivability and increase success rate of the experiments.

Our current model of PT does not require the purchase of any expensive instruments, as any laboratory that is equipped with an epi-fluorescence microscope with a light source (such as mercury lamp, metal halide lamp, or laser of 488 nm wave length) can perform this procedure. In addition, this technique provides control over the size of the infarct by adjusting the aperture size as compared to other SC ischemia models like combined occlusion of aortic, left subclavian and internal mammary artery[25] and modified aortic cross clamping method[26] which are complicated and are extremely invasive. In our model a high speed drill to thin the dorsal surface of vertebra for visualization was chosen as an alternative to laminectomy, method of choice by many laboratories to induce SCI. Laminectomy involves cutting of the vertebrae which may cause excessive hemorrhage due to transection of the vertebral blood vessels and this might obscure the field for imaging. Even though some protocols advise the use of cotton swabs to clear out the excessive bleeding during laminectomy it may result in compression which may cause additional injury to the SC. Further the exposed surface of the spinal cord can come in direct contact with blood and its

constituents as well as sharp edges of the cut bones which can add unnecessary variability to the experiment. Using the current PT model, infarction with different size and depth can be generated by simple manipulation of the intensity of the light source, duration of exposure and area of the exposed surface. Although the current study generated ischemia on the central region of T11 in the SC, this method can also generate infarcts at different locations along rostral-to-caudal as well as lateral direction of the spinal cord, which might benefit understanding the region-specific effect of ischemia on paraplegia. On the other hand, although the illumination is on the surface of spinal cord, the light could penetrate to certain depth in the tissue and the injury can also be induced in the grey matter. As Rose Bengal is distributed in entire circulation system, if the animal species are the same, and the age and weight are similar, we expect consistent lesion will be generated as in cortical ischemia induced by PT.

The other major advantage of PT-induced ischemia is very low mortality of animals. Low mortality means long term survival studies can be carried which might be useful in unraveling the temporal effect of ischemic injury on survival and motor function recovery. This model can also aid in understanding the cellular repair mechanisms which usually occur late in the chronic phase of injury[14,19,27-29]. This model also produces considerable motor function deficits which can be used to assess the efficacy of neuroprotective agents on functional recovery. In addition, this model will also allow the study of pathological changes after SCI such as axonal degeneration and regeneration, neuronal and astrocytic Ca^{2+} signaling and overloading in live mice using two-photon microscopy.

Like all other SCI models, PT is not devoid of drawbacks. The disadvantages of this technique are similar to those seen in cortical PT. Few of the shortcomings include lack of an anatomically clear ischemic penumbra, which is the target of many neuroprotective drugs, and the absence of reperfusion. It is well known that reperfusion following ischemia is characterized by changes like increased production of reactive oxygen species, infiltration of inflammatory cells and increased cytokine production[30-32]. Lack of reperfusion in PT means the changes associated with reperfusion injury in SC will remain difficult to study using this model. However, the advantages of using PT induced ischemia outweigh the disadvantages and this technique provides the researchers with an easy to perform and highly reproducible model of generating SCI in mice.

Disclosures

The authors have nothing to disclose.

Acknowledgements

This work was supported by the National Institutes of Health [Grant no. R01NS069726] and the American Heart Association Grant in Aid Grant [Grant no. 13GRNT17020004] to SD.

References

1. Cadotte, D. W., Fehlings, M. G. Spinal cord injury: a systematic review of current treatment options. *Clin Orthop Relat Res.* **469**, (3), 732-741 (2011).
2. Cheriyan, T., *et al.* Spinal cord injury models: a review. *Spinal Cord.* **52**, (8), 588-595 (2014).
3. Young, W. Secondary injury mechanisms in acute spinal cord injury. *J Emerg Med.* **11**, Suppl 1. 13-22 (1993).
4. Crowe, M. J., Bresnahan, J. C., Shuman, S. L., Masters, J. N., Beattie, M. S. Apoptosis and delayed degeneration after spinal cord injury in rats and monkeys. *Nat Med.* **3**, (1), 73-76 (1997).
5. Soubeyrand, M., *et al.* Effect of norepinephrine on spinal cord blood flow and parenchymal hemorrhage size in acute-phase experimental spinal cord injury. *Eur Spine J.* **23**, (3), 658-665 (2014).
6. Soubeyrand, M., *et al.* Real-time and spatial quantification using contrast-enhanced ultrasonography of spinal cord perfusion during experimental spinal cord injury. *Spine (Phila Pa 1976).* **37**, (22), E1376-E1382 (2012).
7. Mautes, A. E., Weinzierl, M. R., Donovan, F., Noble, L. J. Vascular events after spinal cord injury: contribution to secondary pathogenesis). *Phys Ther.* **80**, (7), 673-687 (2000).
8. Liu, X. Z., *et al.* Neuronal and glial apoptosis after traumatic spinal cord injury. *J Neurosci.* **17**, (14), 5395-5406 (1997).
9. Liu, L., *et al.* An experimental study of cell apoptosis and correlative gene expression after tractive spinal cord injury in rats. *Zhonghua Wai Ke Za Zhi.* **42**, (23), 1434-1437 (2004).
10. Hirose, K., *et al.* Activated protein C reduces the ischemia/reperfusion-induced spinal cord injury in rats by inhibiting neutrophil activation. *Ann Surg.* **232**, (2), 272-280 (2000).
11. Oyinbo, C. A. Secondary injury mechanisms in traumatic spinal cord injury: a nugget of this multiply cascade. *Acta Neurobiol Exp (Wars).* **71**, (2), 281-299 (2011).
12. Guerit, J. M., Dion, R. A. State-of-the-art of neuromonitoring for prevention of immediate and delayed paraplegia in thoracic and thoracoabdominal aorta surgery). *Ann Thorac Surg.* **74**, (5), S1867-S1869 (2002).
13. Schepens, M. A., Heijmen, R. H., Ranschaert, W., Sonker, U., Morshuis, W. J. Thoracoabdominal aortic aneurysm repair: results of conventional open surgery. *Eur J Vasc Endovasc Surg.* **37**, (6), 640-645 (2009).
14. Braeuninger, S., Kleinschnitz, C. Rodent models of focal cerebral ischemia: procedural pitfalls and translational problems. *Exp Transl Stroke Med.* **1**, 8 (2009).
15. Carmichael, S. T. Rodent models of focal stroke: size, mechanism, and purpose. *NeuroRx.* **2**, (3), 396-409 (2005).
16. Dietrich, W. D., Ginsberg, M. D., Busto, R., Watson, B. D. Photochemically induced cortical infarction in the rat. 1. Time course of hemodynamic consequences. *J Cereb Blood Flow Metab.* **6**, (2), 184-194 (1986).
17. Zhang, W., *et al.* Neuronal protective role of PBEF in a mouse model of cerebral ischemia. *J Cereb Blood Flow Metab.* **30**, (12), 1962-1971 (2010).
18. Li, H., Zhang, N., Sun, G., Ding, S. Inhibition of the group I mGluRs reduces acute brain damage and improves long-term histological outcomes after photothrombosis-induced ischaemia. *ASN Neuro.* **5**, (3), 195-207 (2013).

19. Li, H., *et al.* Histological, cellular and behavioral assessments of stroke outcomes after photothrombosis-induced ischemia in adult mice. *BMC Neurosci.* **15**, 58 (2014).
20. Wang, T., Cui, W., Xie, Y., Zhang, W., Ding, S. Controlling the Volume of the Focal Cerebral Ischemic Lesion through Photothrombosis. *American Journal of Biomedical Sciences.* **2**, (1), 33-42 (2010).
21. Schroeter, M., Jander, S., Stoll, G. Non-invasive induction of focal cerebral ischemia in mice by photothrombosis of cortical microvessels: characterization of inflammatory responses. *J Neurosci Methods.* **117**, (1), 43-49 (2002).
22. Boquillon, M., Boquillon, J. P., Bralet, J. Photochemically induced, graded cerebral infarction in the mouse by laser irradiation evolution of brain edema. *J Pharmacol Toxicol Methods.* **27**, (1), 1-6 (1992).
23. Kim, G. W., Lewen, A., Copin, J., Watson, B. D., Chan, P. H. The cytosolic antioxidant, copper/zinc superoxide dismutase, attenuates blood-brain barrier disruption and oxidative cellular injury after photothrombotic cortical ischemia in mice. *Neuroscience.* **105**, (4), 1007-1018 (2001).
24. Schmidt, A., *et al.* Photochemically induced ischemic stroke in rats. *Exp Transl Stroke Med.* **4**, (1), 13 (2012).
25. Lang-Lazdunski, L., *et al.* Spinal cord ischemia. Development of a model in the mouse. *Stroke.* **31**, (1), 208-213 (2000).
26. Wang, Z., *et al.* Development of a simplified spinal cord ischemia model in mice. *J Neurosci Methods.* **189**, (2), 246-251 (2010).
27. Labat-gest, V., Tomasi, S. Photothrombotic ischemia: a minimally invasive and reproducible photochemical cortical lesion model for mouse stroke studies. *J Vis Exp.* (76), (2013).
28. Lu, H., *et al.* Induction and imaging of photothrombotic stroke in conscious and freely moving rats. *J Biomed Opt.* **19**, (9), 96013 (2014).
29. Seto, A., *et al.* Induction of ischemic stroke in awake freely moving mice reveals that isoflurane anesthesia can mask the benefits of a neuroprotection therapy. *Front Neuroenergetics.* **6**, (1), (2014).
30. Bell, M. T., *et al.* Toll-like receptor 4-dependent microglial activation mediates spinal cord ischemia-reperfusion injury. *Circulation.* **128**, (11 Suppl 1), S152-S156 (2013).
31. Smith, P. D., *et al.* The evolution of chemokine release supports a bimodal mechanism of spinal cord ischemia and reperfusion injury. *Circulation.* **126**, (11 Suppl 1), S110-S117 (2012).
32. Jia, Z., *et al.* Oxidative stress in spinal cord injury and antioxidant-based intervention. *Spinal Cord.* **50**, (4), 264-274 (2012).

